JYX
JYVÄSKYLÄN YLIOPISTO
UNIVERSITY OF JYVÄSKYLÄ

This is a self-archived version of an original article. This version may differ from the original in pagination and typographic details.

Author(s): Kuosmanen, Riikka T.; Truong, Khai-Nghi; Rissanen, Kari T.; Sievänen, Elina I.

Title: The Effect of the Side Chain on Gelation Properties of Bile Acid Alkyl Amides

Year: 2021

Version: Published version

Copyright: © 2021 The Authors. Published by Wiley-VCH GmbH.

Rights: CC BY-NC 4.0

Rights url: https://creativecommons.org/licenses/by-nc/4.0/

Please cite the original version:

Kuosmanen, R. T., Truong, K., Rissanen, K. T., & Sievänen, E. I. (2021). The Effect of the Side Chain on Gelation Properties of Bile Acid Alkyl Amides. ChemistryOpen, 10(11), 1150-1157. https://doi.org/10.1002/open.202100245

ChemistryOpen

Research Article
doi.org/10.1002/open.202100245

Chemistry Europe
European Chemical Societies Publishing

The Effect of the Side Chain on Gelation Properties of Bile Acid Alkyl Amides

Riikka T. Kuosmanen, Khai-Nghi Truong, Kari T. Rissanen,* and Elina I. Sievänen*[a]

Six bile acid alkyl amide derivatives were studied with respect to their gelation properties. The derivatives were composed of three different bile acids with hexyl or cyclohexyl side chains. The gelation behaviour of all six compounds were studied for 36 solvents with varying polarities. Gelation was observed mainly in aromatic solvents, which is characteristic for bile-acid-based low molecular weight gelators. Out of 108 bile acid-solvent combinations, a total of 44 gel systems were formed, 28 of which from lithocholic acid derivatives, only two from deoxycholic acid derivatives, and 14 from cholic acid derivatives. The majority of the gel systems were formed from bile acids with hexyl side chains, contrary to the cyclohexyl group, which seems to be a poor gelation moiety. These results indicate that the spatial demand of the side chain is the key feature for the gelation properties of the bile acid amides.

1. Introduction

Research on supramolecular gelation and the gel properties has tremendously increased over the past three decades. The field of supramolecular gels is intriguing because of the multitude of compounds[1,2] and mixtures of compounds[3] which are able to form gels. This ever-expanding library of compounds has provided many fascinating supramolecular gel systems with possible applications in regenerative medicine,[1,4–6] treatment of cancer,[1,7] environmental remediation,[8–12] imaging[1] as well as many others. The formation of the supramolecular gel occurs by immobilization of the solvent through weak interactions, such as hydrogen bonding, π-π-interactions, or metal coordination. A self-assembled network of fibres or other nano- or microstructures is spontaneously formed by the gelator molecules. Because both supramolecular gelation and crystallization arise from nucleation processes,[13] and some gelator molecules have a very strong tendency to form single-crystalline materials, the information obtained from solid-state structures via single crystal X-ray crystallography can shed light on the interactions responsible for the formation of the supramolecular gels. Detailed structural information offers a possibility to draw conclusions on how the structure of the gelator molecule correlates with the self-assembly, i.e. gelation properties. The impact of structure on gelation behaviour has been studied for many types of compounds such as divergent organic salts[14–16] and bile acid derivatives containing amino acid moieties.[17–18]

In the liver, cholesterol is converted to bile acids during complex biosynthetic paths.[19–22] Thus, because bile acids are intrinsic to human bodies, they are biologically and chemically interesting. Bile acids assist in the absorption of lipids and lipid soluble vitamins. On the other hand, defects in the bile acid metabolism or excretion can lead to severe medical conditions. In supramolecular chemistry, bile acids are intriguing starting materials, since they can be relatively easily modified, provide divergent steroidal backbones, and are cheap and easily available starting materials. Bile acids are also amphiphilic, containing hydrophilic and hydrophobic sides, from which the different self-assembly motifs together with chemical and biological properties arise. Hence, bile acids and their derivatives have multiple applications in medicine, for example in treatment of liver diseases[23,24] as well as for diabetes[25–28] and as antimicrobial agents.[29]

During the past fifteen years, a large number of bile acid derivatives have been studied regarding their gelation properties in our research group.[17,18,30–38] Recently, we have been interested in bile acid derivatives which do not have any functional group at their end of the side chain. In this respect, we wondered how the length and the shape (linear or branched) of the functional-group-free side chain affected the gel formation ability of a particular bile acid derivative.

Herein, we report six new bile acid derivatives, crystal structures for five of them, and the studies of their gelation properties. The compounds consist of three different bile acids with a hexyl- or a cyclohexylamide side chain. The gelation studies reveal that the side chain has a marked influence on the gelation ability of the bile acid amides. Clearly, the number of hydroxyl groups on the steroidal skeleton of the compound has an effect on gelation, verifying previous observations.[17,18,30–38]

[a] R. T. Kuosmanen, Dr. K.-N. Truong, Prof. Dr. K. T. Rissanen, Dr. E. I. Sievänen
Department of Chemistry
University of Jyvaskyla
P.O. Box 35, 40014 Jyväskylä (Finland)
E-mail: kari.t.rissanen@jyu.fi
elina.i.sievanen@jyu.fi

Supporting information for this article is available on the WWW under https://doi.org/10.1002/open.202100245

© 2021 The Authors. Published by Wiley-VCH GmbH. This is an open access article under the terms of the Creative Commons Attribution Non-Commercial License, which permits use, distribution and reproduction in any medium, provided the original work is properly cited and is not used for commercial purposes.

2. Results and Discussion

2.1. Synthesis

The bile acid amides **1**–**6** were synthesized through the route presented in Scheme 1, frequently utilized by our research group.[17,18,30–36] Compounds **1**–**6** were purified either by column chromatography or by recrystallization methods. The isolated yields varied from 11% to 54%. The syntheses and characterisation details for compounds **1**–**6** can be found in the Supporting Information.

2.2. Solid-State Structures

Single crystals of the amides **1**–**5** suitable for X-ray diffraction were obtained by slow evaporation of either their acetonitrile or 1,4-dioxane solutions. Unfortunately, not all of the crystallization attempts were successful. Despite numerous attempts, compound **6** was only obtained as a gel or amorphous powder. The solid-state structures of compounds **1**–**5** are depicted in Figure 1.

Compound **2** crystallized in the highly symmetrical tetragonal space group $P4_3$, whereas all the other hexyl and cyclohexyl derivatives, similar to the previously studied lithocholyl, deoxycholyl, and cholyl amides bearing ethyl,[34] propyl, butyl, and isopentyl side chains,[33] crystallize in the monoclinic space group $P2_1$.

As the previously studied ethyl, propyl, butyl, and isopentyl derivatives,[33,34] also the current series of hexyl- and cyclohexyl amides **1**–**5** crystallized without solvent molecules. Within the series of bile acid alkyl amides, bile acid-solvent interactions have hitherto only been observed for the *N*-ethyldeoxycholamide and *N*-ethylcholamide.[34] In addition to stabilizing the crystal lattice, the co-crystallized acetonitrile molecules had a significant influence on the structure of the side chain orientation of the respective bile acid, as can been seen in Figure 2 (red capped stick models).

In amides **1**, **2**, **4**, and **5**, intermolecular bile acid-bile acid interactions, i.e. O–H···O and N–H···O hydrogen bonds between hydroxyl and amide groups, are responsible for forming the typical ordered 1D bilayered structures (Figure 3(a) and Figures S8–S12).[33,39–41] Differing from the other derivatives, compound **3** forms a 2D hydrogen-bonded polymer where neighbouring 1D bilayered, tubular assemblies are interconnected through N–H···O hydrogen bonds as illustrated in Figure 3(c) – black broken lines. Since compound **3** crystallizes not with one molecule but two crystallographically independent molecules in the asymmetric unit, the *N*-alkyl side chains are oriented in different conformations (Figure S5) and are engaged in hydrogen bonding different to what had hitherto been observed.

The infinite 1D bilayer structure observed in virtually all bile acid amide structures[33,34] is stabilized by several intermolecular O–H···O and N–H···O interactions between the hydroxyl groups at the 3α(/7α/12α)-position(s) as well as by interactions between the carbonyl and N–H groups in the side chains of the bile acid amides. This known motif was observed for one of the

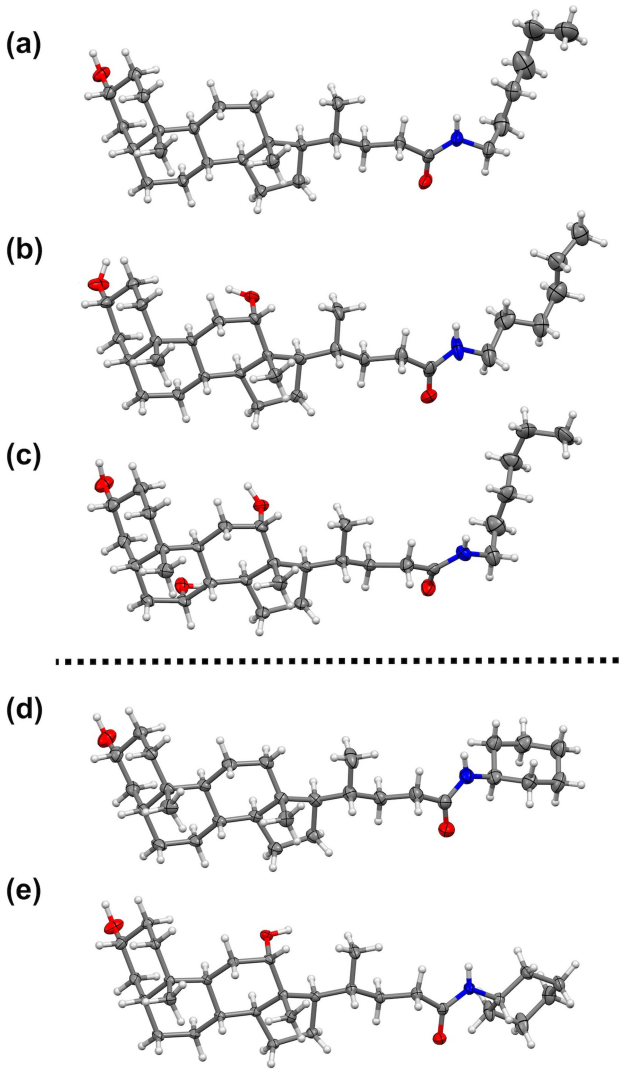

Figure 1. The X-ray structures of **1**–**5**: (a) *N*-hexyllithocholamide, **1**, (b) *N*-hexyldeoxycholamide, **2**, (c) *N*-hexylcholamide, **3**, (d) *N*-cyclohexyllithocholamide, **4**, and (e) *N*-cyclohexyldeoxychol-amide, **5**. Displacement ellipsoids are drawn at the 50% probability level. Atom sites with minor occupancies have been omitted for clarity. Color code: grey (C), white (H), red (O), and blue (N).

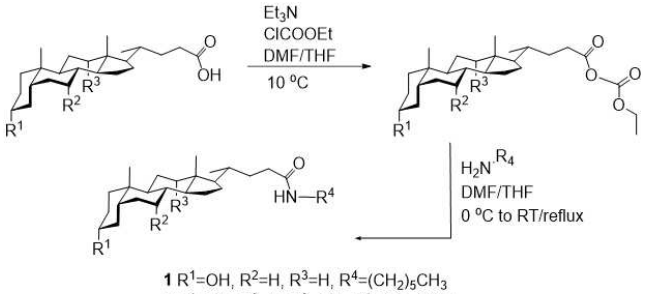

1 R^1=OH, R^2=H, R^3=H, R^4=$(CH_2)_5CH_3$
2 R^1=OH, R^2=H, R^3=OH, R^4=$(CH_2)_5CH_3$
3 R^1=OH, R^2=OH, R^3=OH, R^4=$(CH_2)_5CH_3$
4 R^1=OH, R^2=H, R^3=H, R^4=C_6H_{11}
5 R^1=OH, R^2=H, R^3=OH, R^4=C_6H_{11}
6 R^1=OH, R^2=OH, R^3=OH, R^4=C_6H_{11}

Scheme 1. The synthetic route to bile acid derivatives **1**–**6**.

© 2021 The Authors. Published by Wiley-VCH GmbH

molecules of **3**. The other molecule in the X-ray structure of **3** forms the bilayered structures only with O–H···O hydrogen bonds. The "free" N–H groups act as linkers between the bilayers and are stabilized by N–H···O(carbonyl) interactions with d(N···O) = 3.008 Å. The polar and apolar layers alternate along the *b*-axis (Figure 3(d)).

Compared to the previously studied ethyl, propyl, butyl, and isopentyl derivatives,[33,34] the *n*-hexyl and cyclohexyl groups in compounds **1**–**5** impart flexibility with high degrees of conformational freedom (Figures S4 and S5). In addition, the flexibility of the alkyl chains increases with the number of hydroxyl groups attached to the steroidal backbone (Figure 2). Hirshfeld surface analyses[42–45] for the crystal structures indicate that the bilayers form a compact 3D crystal lattice through a high percentage of H···H contacts (Table S4 and Figures S13–17, Supporting Information). Surprisingly, the highest percentage of H···H contacts was observed for **2**, *N*-hexyldeoxycholamide, which contrasts the previously observed behavior where the H···H interactions decrease with an increasing number of hydroxyl groups attached to the steroidal backbone (Table S4). The X-ray structures of *N*-hexyldeoxycholamide, **2**, and *N*-cyclohexyldeoxycholamide, **5**, do not offer any apparent molecular or intermolecular-interaction-based explanation (see Hirshfeld surface analysis, Table S4) on not forming gels similarly to the OH-group-containing lithocholamides and the three OH-group-containing hexylcholamides (Table 1). Despite very similar molecular conformations and packing in the crystal lattice (Figures 1 and 2), the likely cause for the non-gelation is either too low or too high solubility in the target solvent.

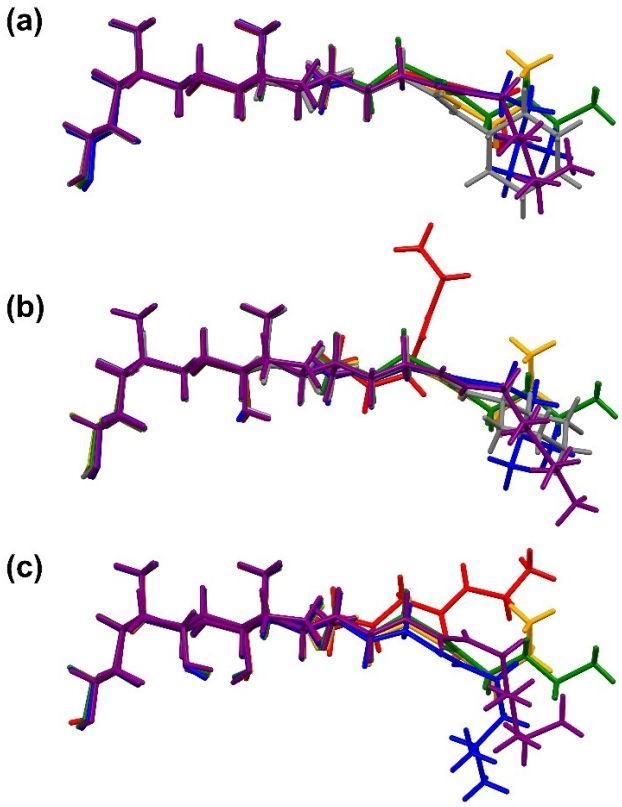

Figure 2. Overlay of the X-ray crystal structures of all (a) lithocholamide, (b) deoxycholamide, and (c) cholamide derivatives shown in capped stick model. Color code: red (*N*-ethyl),[34] gold (*N*-propyl),[33] green (*N*-butyl),[33] blue (*N*-isopentyl),[33] grey (*N*-cyclohexyl), and purple (*N*-hexyl). Co-crystallized solvent molecules as well as atom sites with minor occupancies have been omitted for clarity.

2.3. Gelation Studies

The results of the gelation test of compounds **1**–**6** conducted in 36 solvents were in good congruence with the results obtained previously in our group.[17,18,30–36] Most of the gel systems were formed in aromatic solvents and are presented in Table 1. More detailed information on the gelation experiments can be found in the Supporting Information. A total of 44 gel systems were formed, 28 of which by lithocholic acid derivatives (compounds **1** and **4**), two by a deoxycholic acid derivative (compound **2**), and 14 by cholic acid derivatives (compounds **3** and **6**). No gelation was observed in alcohols or chlorinated solvents with the exception of chlorobenzene.

The deoxycholic acid derivative **5**, containing a cyclohexyl side chain, did not form any gels. The other deoxycholic acid derivative with the hexyl side chain (compound **2**), however, formed two gel systems. This was unexpected, since deoxycholic acid derivatives do not usually self-assemble into gels as previously observed.[17,18,30–36] The majority of the gel systems were formed by lithocholic acid derivatives **1** and **4**. Compound **1** was observed to form gel systems in the largest number of solvents. The cholic acid derivative **3** was the only compound exclusively forming flawless gels, half of which started to degrade after four hours. According to our previous studies,[33,34] lithocholic acid derivatives have been more efficient gelator molecules, whereas in this study, mostly partial gels were obtained. For example, in the case of compound **1** which

Table 1. Solvents in which compounds **1**–**6** formed gel systems.

Solvent	1	2	3	4	5	6
Benzene	**PG**	**PG^s**	**G^f**	–	–	**G^f**
Toluene	**G^f**	–	**G^f**	**PG^s**	–	**PG^s**
Ethylbenzene	**PG**	–	–	**PG**	–	**G^s**
o-Xylene	**PG**	–	**G^f**	**PG**	–	**G^{es}**
m-Xylene	**G^f**	–	–	**PG**	–	**PG^s**
p-Xylene	**G^f**	–	–	**PG**	–	**PG^s**
Mesitylene	**PG**	–	–	–	–	–
tert-Butylbenzene	**G^f**	–	**G^f**	**PG**	–	–
Cumene	**PG**	–	–	**PG**	–	–
Chlorobenzene	–	–	**G^s**	–	–	**G^{es}**
Anisole	**PG^s**	–	**G^s**	–	–	**G^{es}**
ACN	**G^f**	–	–	–	–	–
Ethyl acetate	**G^f**	–	–	**PG**	–	–
n-Hexane	**G^f**	–	–	**PG**	–	–
Diethyl ether	**PG^f**	–	–	–	–	–
DMSO	–	–	–	**PG**	–	–
Formamide	–	–	–	**PG**	–	–
Ethylene glycol	–	**G^s**	–	**PG**	–	–
Cyclohexene	**PG**	–	–	**G**	–	–

Abbreviations: **G^f** (gel formed under 30 min), **G** (gel formed within an hour), **G^s** (gel formed after 1 day), **G^{es}** (gel formed extremely slowly, after months), **PG^f** (partial gel formed in 30 min), **PG** (partial gels formed within an hour), **PG^s** (partial gel formed after 1 day), and "–" (no gel).

© 2021 The Authors. Published by Wiley-VCH GmbH

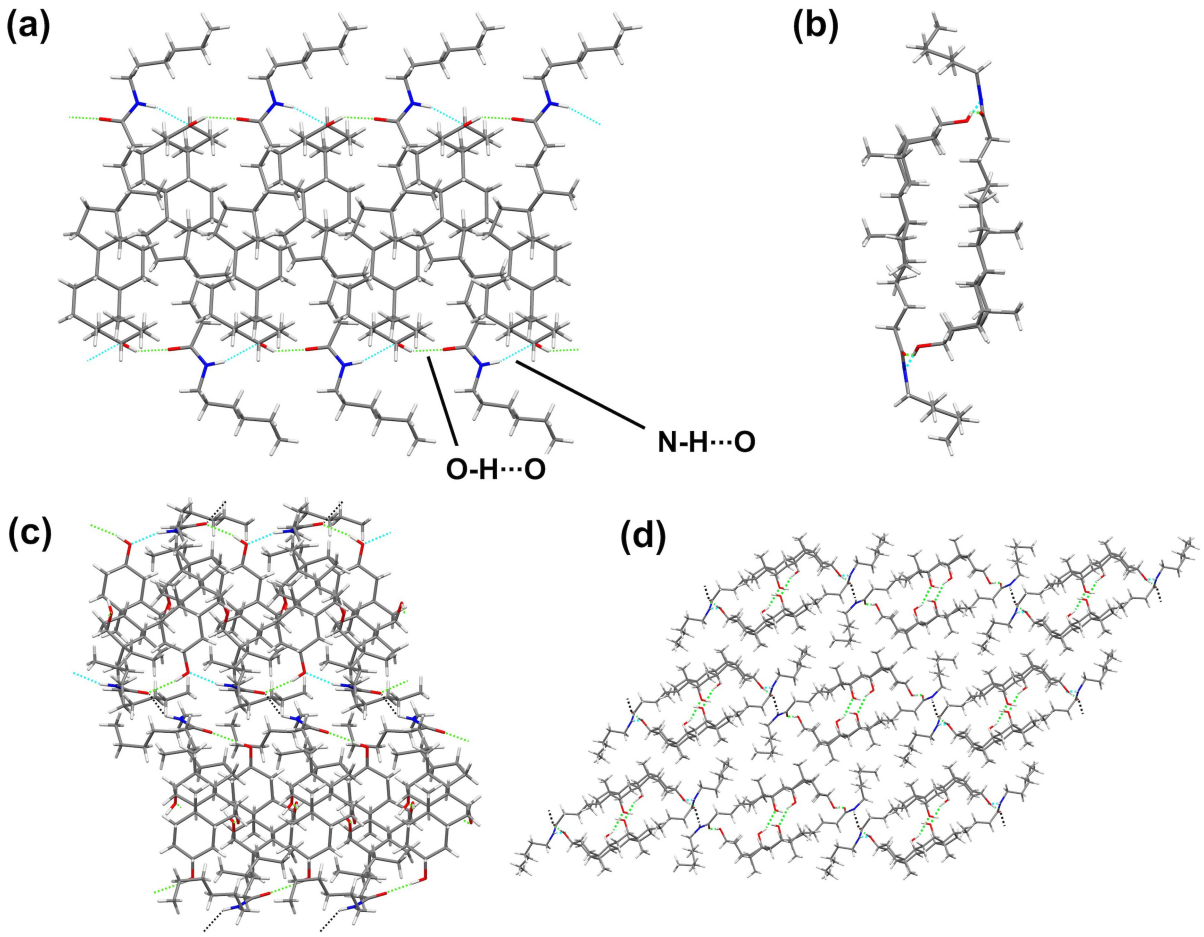

Figure 3. The 1D hydrogen-bonded polymer viewed along the *a*-axis (a) and the tubular assembly viewed along the *b*-axis of **1** (b), 2D hydrogen-bonded polymer viewed along the *a*-axis (c) and along the *b*-axis of **3** (d) in capped stick model. Atom sites with minor occupancies have been omitted for clarity. Broken lines represent N–H·O (turquoise and black) and O–H·O (green) hydrogen bonding. Color code: grey (C), white (H), red (O), and blue (N).

formed the largest number of gel systems, eight of the fifteen gels formed were partial.

The time of the gel formation was exceptionally short for compound **3** in most of the solvents: four out of the six gels formed in only three minutes. On the other hand, in chlorobenzene and anisole, the gel formation took four days. There appears to be a correlation between the temporal stability of the gel and the formation time: slowly formed gels were stable, whereas extremely quickly formed gels started to collapse within four hours (except the gel in *tert*-butylbenzene). A similar phenomenon was not observed with compound **6**, where both the quickly and the slowly formed gels were equally stable. Compound **1** self-assembled into gels fast as well, but the gelation time was considerably slower (over fifteen minutes) when compared with compound **3**. When comparing the melting points of the benzene gels of compounds **1**, **2**, **3**, and **6**, differences were observed. The benzene gels of compounds **1**–**3** had similar melting points ranging from 64 °C to 69 °C. Hence, the compound or the formation time of the gel did not have a pronounced effect on the melting point. However, the benzene gel of compound **6** deviated from this trend as it had a significantly higher melting point (80 °C). In the case of compound **6**, melting points of the gels were also determined in differing solvents. The gels in chlorobenzene, *o*-xylene and anisole exhibited lower melting points ranging from 70 °C to 76 °C than those observed for the corresponding benzene gel. The highest melting point was observed for the ethylbenzene gel of compound **6** (94 °C).

When considering the melting points of the gels in different solvents and the formation time of the gels, the least stable ones corresponded to the most slowly formed gels.

An interesting congruence with respect to the gelator molecule and the solvent was observed, showing that the lithocholic acid derivatives (**1** and **4**) formed gels when having a complimentary structure of the side chain and the solvent. Compound **1**, with its linear hexyl side chain, formed a gel in *n*-hexane, whereas compound **4** only formed a partial gel. In cyclohexene, compound **4**, with its cyclohexyl side chain, formed a gel and compound **1** self-assembled into a partial gel.

Differences in the appearance and consistence of the gel systems in different solvents were also observed. Compound **1** produced cleavable, bright gels in benzene and cyclohexene, whereas the gels in acetonitrile and diethyl ether were clearly fibrous. The gel of compound **4** in toluene was also fibrous.

© 2021 The Authors. Published by Wiley-VCH GmbH

Gels in cumene were constructed of small spheres in the cases of compounds **1** and **4**. In addition, the gel of compound **4** in cyclohexene also consisted of spheres. The gels of compound **2** in benzene and ethylene glycol were ductile, as was the gel of compound **3** in benzene. Especially in the case of compound **3** in benzene, the gel appeared extremely stretchy. The gel formed by compound **6** in benzene, for one, resembled a jelly. All the gel systems were qualitatively stable; each either maintaining its shape or returning to a smooth-surfaced gel after being disturbed with a spatula. This was surprising, since in our previous studies the gels collapsed immediately when disturbed.[33,34]

Similar to our previous studies,[33,34] all the gels in the current study were thixotropic by nature.

Kamlet-Taft solvent parameters can be used in determining the solvents' properties.[46–48] They include three parameters that can be utilized in the analysis of solvent interactions in gel systems. The α- and β-parameters describe the hydrogen-bond-donating and accepting ability of the solvent, respectively. The third parameter, the π*-parameter, refers to the polarizability of the solvent. In the current study, all solvents in which gels or partial gels were formed were analyzed with respect of the three Kamlet-Taft parameters (see Figure 4). The gelating and non-gelating solvents are divided by a vertical line in Figure 4.

In our previous studies,[36] the α-parameter (hydrogen bond donor ability) was observed to be an important Kamlet-Taft parameter effecting the immobilization of the solvent by a gelating compound. The value was zero for most of the gel-forming solvents. In this study, the α-parameter exhibited similar properties (Figure 1) as it was zero for all the gel-forming solvents, with the exception of acetonitrile (0.19), formamide (0.71), and ethylene glycol (0.90). The majority of the β-parameter values (hydrogen bond acceptor ability) were in accordance with previous studies of bile acid derivatives having moderate values from 0.10 to 0.31.[34] The gelating solvents diethyl ether, ethyl acetate, dimethyl sulphoxide, and ethylene glycol have higher β-parameter values (0.47, 0,45, 0.76, and 0.52, respectively). This differs from our previous results,[36] where a higher β-value seemed to completely prevent gelation. The lack of the functional group at the end of the aliphatic side chain probably enables the gel formation in a larger versatility of solvents. On the other hand, the steroidal backbone may also play an important role: in the current study, lithocholic acid, deoxycholic acid, and cholic acid backbones were used, whereas in the previous one,[36] instead of cholic acid, chenodeoxycholic acid was used. When comparing the π*-parameter (polarizability) values, acetonitrile, formamide, and ethylene glycol again stand out with significantly higher values, as do chlorobenzene and anisole. For all the other gelating solvents, the value of the π*-parameter varies between 0 and 0.56.

When looking into the Kamlet-Taft parameters regarding the chlorinated solvents, an interesting difference is observed. Chlorobenzene, in which gels were formed, is clearly divergent from chloroform and dichloromethane, which did not induce gel formation. Chloroform and dichloromethane both possess a slightly higher hydrogen bond donor ability (α-value) than chlorobenzene. The hydrogen bond acceptor ability (β-value), however, seems to be a more significant factor for gelation within chlorinated solvents used in this study, since chlorobenzene has the highest value of the three. The same observation applies to the polarizability of the solvent (π*-value), which means that the solvation of peripheral groups of the gelator molecule and the fiber-fiber interactions play a major role in gel formation in chlorinated solvents.

When comparing the aromatic solvents in which gels were formed (excluding chlorobenzene), anisole seems different from the other aromatic solvents at first glance. Anisole has markedly higher β- and π*-values than other the aromatic solvents, but the α value is zero, as is the case with all the other aromatic solvents. When the ratio of β/π* is calculated (Table S2, Supporting Information), all aromatic solvents, however, show similar ratios around 0.30.

Compounds **1**–**6** were highly soluble in alcohols, meaning that gelation was not observed. All Kamlet-Taft parameters are,

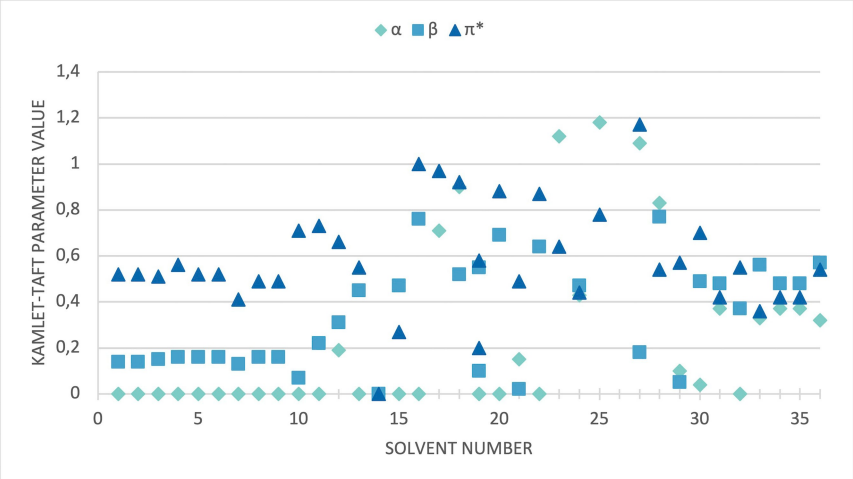

Figure 4. Kamlet-Taft parameters (α, β, and π*) for gel-forming (1–19) and not gel-forming (20–36) solvents (Table 1 and Supporting Information). The vertical line divides the gel-forming and the non-gel-forming solvents.

© 2021 The Authors. Published by Wiley-VCH GmbH

in general, in the same range for the alcohols, which leads to the conclusion that solvents which possess relatively equal hydrogen bond donor and acceptor abilities are not good solvents for gelation with bile acid amides.

2.4. Morphology

In the SEM images of the selected dried gel systems (xerogels), mostly fibrous structures were seen. In the fibrous gel networks, the larger fibres were observed to have formed from thinner fibres (Figure S2).

The gels of compounds **3** and **6** formed in benzene were divergent: smooth ball-shaped structures were observed (Figure 5(a) and (b), respectively). For compound **3**, the diameter of the spheres varied from 1.3 μm to 3.9 μm. In the case of compound **6**, the spheres were fused https://www.merriam-webster.com/dictionary/elided and the gel appeared as dough-like in the SEM images. The spherical structures were uniform in size, the average diameter being 665 nm. The gel of compound **3** in benzene was extraordinary by its physical appearance also, because the gel was very elastic and stretchy.

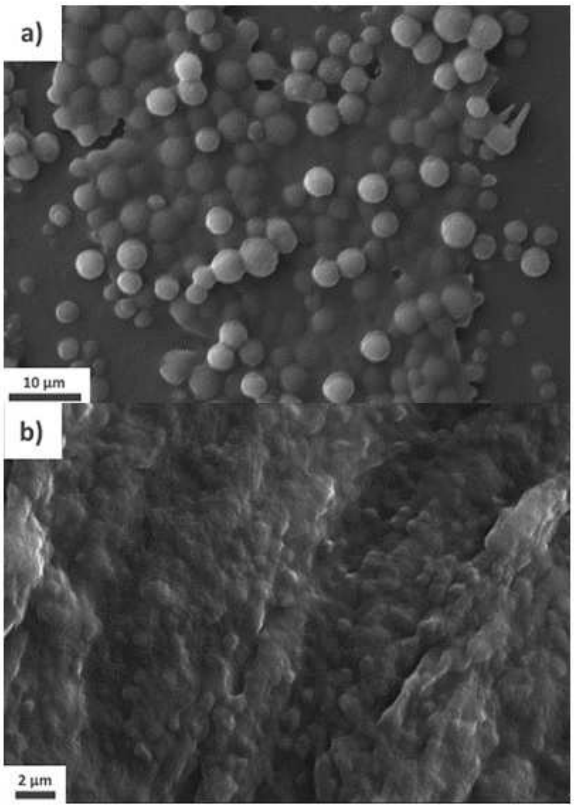

Figure 5. SEM images of xerogels formed from compound **3** (a), and compound **6** (b) in benzene.

Compounds **1** and **2** in benzene and compound **4** in toluene formed a fibrous gel network consisting of uniform-looking fibres (Figure 6). The width and length of the fibres varied within each system. The longest fibres were formed by compound **4** (from 61 μm to 775 μm) and the shortest fibres by compound **2** (from 12 μm to 242 μm). In the case of compound **1**, the length of the fibres varied from 19 μm to 376 μm. When comparing the width of the fibres, compound **4** possessed the thickest fibres (from 1.5 μm to 7.8 μm) and compounds **1** (from 654 nm to 6.6 μm) and **2** (from 732 nm to 4.7 μm) thinner ones. The texture of the gels formed in benzene and toluene was different. The gel formed by compound **4** in benzene was clearly fibrous (already to the naked eye), whereas the gel of **1** in benzene was cleavable. The gel formed by compound **2**, on the other hand, was clearly more ductile. It seems that the smaller and more even-sized fibres give rise to a more elastic gel as illustrated by compound **2** in benzene, and fibres with more versatility in size and shape produce less elastic gels as exemplified by compound **1** in benzene.

When inspecting the gel in acetonitrile and the partial gel in diethyl ether formed by compound **1** at a macroscopic level, both were fibrous. In the SEM images (Figures S1(a) and (b), respectively), both consisted of fibres in various sizes. Particularly, in acetonitrile, the gel network resembled a mixture of pieces of fettuccine and tagliatelle pasta. The length of the fibres varied from 24 μm to 244 μm, and the width from 1.5 μm to 6 μm. The average size of the plate-like structures amounted to approximately $37 \times 66\ \mu m^2$. In the partial gel formed in diethyl ether, the length of the fibres varied between 9.3 μm and 220 μm and the width from 863 nm to 13.5 μm, respectively.

The gels formed by compounds **1** and **4** in cyclohexene (Figures S1(c) and (d), respectively) and cumene (Figures S1(e) and (f), respectively) resembled each other. In the case of compound **4**, a correlation between the appearance of the gel and the structures seen in SEM images was observed. In both solvents, compound **4** formed a gel system consisting of

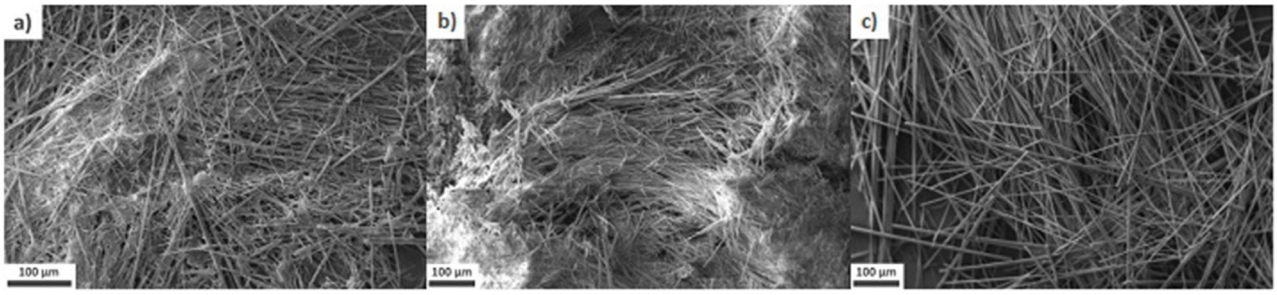

Figure 6. SEM images of compound **1** in benzene (a), compound **2** in benzene (b), and compound **4** in toluene (c).

© 2021 The Authors. Published by Wiley-VCH GmbH

spherical shapes. In the SEM images, the gel network fibres were observed to form larger spherical structures. In cyclohexene, the length of the fibres was 27–314 μm and the width was measured to 309 nm–2.6 μm, whereas in cumene, the length of the fibres varied from 3.6 μm to 274 μm and the width ranged from 860 nm to 9.8 μm, respectively. The partial gel in cyclohexene formed by compound **1** was cleavable, whereas the partial gel in cumene consisted of spherical structures. Both of the gel systems were observed to consist of evenly distributed fibres with various sizes. In cyclohexene, the length of the fibres was 55–378 μm and the width was found at 1.4–13.6 μm. The partial gel formed in cumene by compound **1** resembled the gel formed in acetonitrile by the same compound, although in cumene, the fibres were smaller. The length of the fibres in cumene was 570 nm–14.8 μm and the width was measured to 7.9–239 μm, respectively.

The gel formed by compound **2** in ethylene glycol (Figure S1(g)), which formed extremely slowly, consisted of beam-like short fibres of various sizes. Their width varied from 1.7 μm to 6.3 μm, and their length ranged from 3.5 μm to 43 μm. The texture of the gel was notably more viscous and it stretched more than the other gel systems studied, an exception being compound **3** in benzene.

3. Conclusions

Compound **1** was clearly the most effective gelator molecule in the series of the six bile acid derivatives investigated within this study. Surprisingly, also a compound with deoxycholic acid backbone (**2**) formed gels. This has rarely been observed before. When comparing the number of the gel systems formed, the lithocholic acid-based compounds **1** and **4** formed the majority of the gel systems. The cholic acid derivative **3**, on the other hand, was the only compound, which exclusively formed flawless gels. This is speculated to be due to the ability of compound **3** to form hydrogen-bonded polymers, as was observed in the solid-state studies.

When comparing the compounds with respect to their side chains (linear hexyl side chains in compounds **1** and **3** and cyclohexyl side chains in compounds **4** and **6**), compounds with the linear hexyl side chain were clearly more effective gelators than compounds with the cyclohexyl side chain. Moreover, compound **2** with the deoxycholyl skeleton bearing the linear hexyl side chain formed gels, whereas the corresponding compound **5**, containing a cyclohexyl side chain, formed no gel systems.

The gel systems formed in this study were qualitatively more stable than gel systems produced in our previous studies.[33,34] They were, for example, stable against mechanical stimulus: when disturbed with a spatula, they maintained their shape or returned to a smooth-surfaced gel. In our previous studies,[33,34] the gel systems collapsed immediately after being mechanically disturbed. Previously studied bile acid alkyl amides bearing shorter or branched side chains (butylamides and *iso*-pentylamides, respectively) were observed to form a larger number of gel systems[33] than the currently studied **1**–**6**. Bile acid alkyl amides with even shorter side chains (ethylamides and propylamides)[33,34] were less effective gelators and the gels also decomposed easily. The effectiveness of gelation should thus be evaluated by taking into account not only the number of gels formed but also the qualitative stability of the gel.

The effect of an even larger branched or cyclic side chain or a longer alkyl group on the gelation process would be fascinating to study in the future, because the length and size of the side chain seems to have a major effect on the stability of the gel systems as observed in this study. These investigations could provide a step towards more accurate design of gelator molecules for desired purposes.

Experimental Section

Details of the syntheses, compound characterizations, and gelation studies are given in the Electronic Supporting Information. Deposition Number(s): 2085751 (for **1**), 2085752 (for **2**), 2085753 (for **3**), 2085754 (for **4**), 2085755 (for **5**) contains the supplementary crystallographic data for this paper. These data are provided free of charge by the joint Cambridge Crystallographic Data Centre and Fachinformationszentrum Karlsruhe Access Structures service.

Acknowledgements

University of Jyvaskyla is acknowledged for financial support. The authors are grateful for Ms. Essi Pyykkö, Ms. Jasmin Kujala and B.Sc. Saana Rekola for synthetic work. Lab. Tech. Johanna Hiidenheimo is thanked for MS measurements and Lab. Tech. Hannu Salo for SEM micrographs.

Conflict of Interest

The authors declare no conflict of interest.

Data Availability Statement

The data that support the findings of this study are available in the supplementary material of this article.

Keywords: bile acid amides · intermolecular interactions · solvent influence · supramolecular gels · X-ray crystallography

[1] X. Du, J. Zhou, J. Shi, B. Xu, *Chem. Rev.* **2015**, *115*, 13165–13307.
[2] R. Kuosmanen, K. Rissanen, E. Sievänen, *Chem. Soc. Rev.* **2020**, *49*, 1977–1998.
[3] L. E. Buerkle, S. J. Rowan, *Chem. Soc. Rev.* **2012**, *41*, 6089–6102.
[4] J. Hoque, N. Sangaj, S. Varghese, *Macromol. Biosci.* **2019**, *19*, 1800259.
[5] A. K. Patterson, D. K. Smith, *Chem. Commun.* **2020**, *56*, 11046–11049.
[6] A. J. Feliciano, C. van Blitterswijk, L. Moroni, M. B. Baker, *Acta Biomater.* **2021**, *124*, 1–14.
[7] X. Ren, N. Wang, Y. Zhou, A. Song, G. Jin, Z. Li, Y. Luan, *Acta Biomater.* **2021**, *124*, 179–190.

© 2021 The Authors. Published by Wiley-VCH GmbH

[8] S. Marullo, C. Rizzo, N. T. Dintcheva, F. Giannici, F. D'Anna, *J. Colloid Interface Sci.* **2018**, *517*, 182–193.
[9] J. Y. C. Lim, S. S. Goh, S. S. Liow, K. Xue, X. J. Loh, *J. Mater. Chem. A* **2019**, *7*, 18759–18791.
[10] W. J. Peveler, H. Packman, S. Alexander, R. R. Chauhan, L. M. Hayes, T. J. Macdonald, J. K. Cockcroft, S. Rogers, D. G. A. L. Aarts, C. J. Carmalt, I. P. Parkin, J. C. Bear, *Soft Matter* **2018**, *14*, 8821–8827.
[11] B. O. Okesola, D. K. Smith, *Chem. Soc. Rev.* **2016**, *45*, 4226–4251.
[12] C. Rizzo, S. Marullo, P. R. Campodonico, I. Pibiri, N. T. Dintcheva, R. Noto, D. Millan, F. D'Anna, *ACS Sustainable Chem. Eng.* **2018**, *6*, 12453–12462.
[13] A. Dawn, M. Mirzamani, C. D. Jones, D. S. Yufit, S. Qian, J. W. Steed, H. Kumari, *Soft Matter* **2018**, *14*, 9489–9497.
[14] F. D'Anna, C. Rizzo, P. Vitale, G. Lazarra, R. Noto, *Soft Matter* **2014**, *10*, 9281–9292.
[15] F. D'Anna, P. Vitale, F. Ferrante, S. Marullo, R. Noto, *ChemPlusChem* **2013**, *78*, 331–342.
[16] C. Rizzo, F. D'Anna, R. Noto, M. Zhang, R. G. Weiss, *Chem. Eur. J.* **2016**, *22*, 11269–11282.
[17] V. Noponen, Nonappa, M. Lahtinen, A. Valkonen, H. Salo, E. Kolehmainen, E. Sievänen, *Soft Matter* **2010**, *6*, 3789–3796.
[18] V. Noponen, H. Belt, M. Lahtinen, A. Valkonen, H. Salo, J. Ulrichová, A. Galandáková, E. Sievänen, *Steroids* **2012**, *77*, 193–203.
[19] A. F. Hofmann, L. R. Hagey, *Cell. Mol. Life Sci.* **2008**, *65*, 2461–2483.
[20] O. Martínez-Augustin, F. S. de Medina, *World J. Gastroenterol.* **2008**, *14*, 5630–5640.
[21] M. C. di Gregorio, J. Cautela, L. Galantini, *Int. J. Mol. Sci.* **2021**, *22*, 1–23.
[22] B. L. Shneider, *J. Pediatr. Gastroenterol. Nutr.* **2001**, *32*, 407–417.
[23] A. Asgharpour, D. Kumar, A. Sanyal, *Hepatol. Int.* **2015**, *9*, 527–533.
[24] T. Ikegami, A. Honda, *Hepatol. Res.* **2018**, *48*, 15–27.
[25] C. Rajani, W. Jia, *Front. Med.* **2018**, *12*, 608–623.
[26] J. A. González-Regueiro, L. Moreno-Castañeda, M. Uribe, N. C. Chávez-Tapia, *Ann. Hepatol.* **2017**, *16*, 15–20.
[27] B. Staels, F. Kuipers, *Drugs* **2007**, *67*, 1383–1392.
[28] R. A. Haeusler, B. Astiarraga, S. Camastra, D. Accili, E. Ferrannini, *Diabetes* **2013**, *62*, 4184–4191.
[29] C. Lin, Y. Wang, M. Le, K. F. Chen, Y. G. Jia, *Bioconjugate Chem.* **2021**, *32*, 395–410.
[30] V. Noponen, S. Bhat, E. Sievänen, E. Kolehmainen, *Mater. Sci. Eng. C* **2008**, *28*, 1144–1148.
[31] V. Noponen, A. Valkonen, M. Lahtinen, H. Salo, E. Sievänen, *Supramol. Chem.* **2013**, *25*, 133–145.
[32] V. Noponen, K. Toikkanen, E. Kalenius, R. Kuosmanen, H. Salo, E. Sievänen, *Steroids* **2015**, *97*, 54–61.
[33] R. Kuosmanen, R. Puttreddy, K. Rissanen, E. Sievänen, *Chem. Eur. J.* **2018**, *24*, 18676–18681.
[34] R. Kuosmanen, R. Puttreddy, R. M. Willman, I. Äijäläinen, A. Galandáková, J. Ulrichová, H. Salo, K. Rissanen, E. Sievänen, *Steroids* **2016**, *108*, 7–16.
[35] M. Löfman, M. Lahtinen, M. Pettersson, E. Sievänen, *Colloids Surf. A* **2015**, *474*, 18–28.
[36] M. Löfman, M. Lahtinen, K. Rissanen, E. Sievänen, *J. Colloid Interface Sci.* **2015**, *438*, 77–86.
[37] M. Löfman, J. Koivukorpi, V. Noponen, H. Salo, E. Sievänen, *J. Colloid Interface Sci.* **2011**, *360*, 633–644.
[38] K. Ahonen, M. K. Lahtinen, M. S. Löfman, A. M. Kiesilä, A. M. Valkonen, E. I. Sievänen, Nonappa, E. T. Kolehmainen, *Steroids* **2012**, *77*, 1141–1151.
[39] Y. Hishikawa, R. Watanabe, K. Sada, M. Miyata, *Chirality* **1998**, *10*, 600–618.
[40] N. Yoswathananont, K. Sada, K. Nakano, K. Aburaya, M. Shigesato, Y. Hishikawa, K. Tani, N. Tohnai, M. Miyata, *Eur. J. Org. Chem.* **2005**, 5330–5338.
[41] K. Nakano, K. Sada, Y. Kurozumi, M. Miyata, *Chem. Eur. J.* **2001**, *7*, 209–220.
[42] M. A. Spackman, J. J. McKinnon, *CrystEngComm* **2002**, *4*, 378–392.
[43] J. J. McKinnon, M. A. Spackman, A. S. Mitchell, *Acta Crystallogr. Sect. B* **2004**, *60*, 627–668.
[44] J. J. McKinnon, D. Jayatilaka, M. A. Spackman, *Chem. Commun.* **2007**, 3814–3816.
[45] M. A. Spackman, D. Jayatilaka, *CrystEngComm* **2009**, *11*, 19–32.
[46] Y. Lan, M. G. Corradini, R. G. Weiss, S. R. Raghavan, M. A. Rogers, *Chem. Soc. Rev.* **2015**, *44*, 6035–6058.
[47] M. J. Kamlet, J.-L. M. Abboud, M. H. Abraham, R. W. Taft, *J. Org. Chem.* **1983**, *48*, 2877–2887.
[48] W. Edwards, C. A. Lagadec, D. K. Smith, *Soft Matter* **2011**, *7*, 110–117.

Manuscript received: October 26, 2021
Revised manuscript received: November 2, 2021

© 2021 The Authors. Published by Wiley-VCH GmbH